Med Ultrason 2024, Vol. 26, no. 3, 316-329

Contribution of MicroFlow imaging in the diagnosis of cystic artery pseudoaneurysm including weak turbulent flow

Isil Basara Akin, Canan Altay, Aytaç Gülcü, Süleyman Men

Department of Radiology, Dokuz Eylul University School of Medicine, Izmir, Turkey

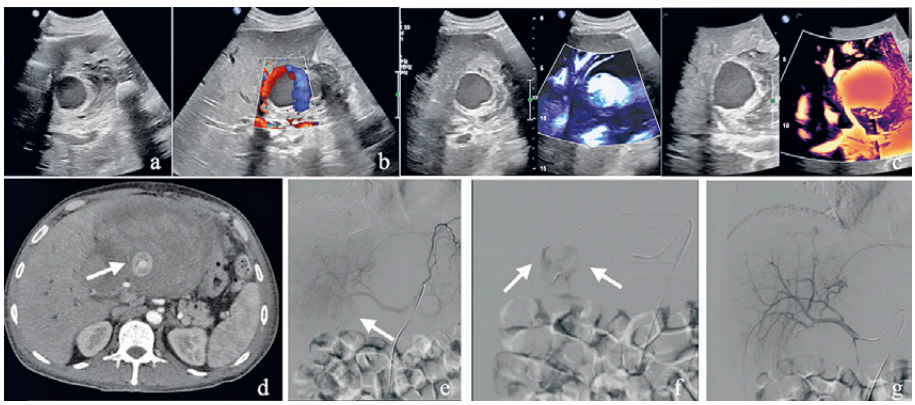

Fig 1. a. B-mod US; b. Doppler US; c. MicroFlow and HighFlow d. CTA images reveal cystic artery pseudoaneurysm. MicroFlow and HighFlow images show prominent vascular filling whereas Doppler US shows no filling; e,f,g. Pseudoaneurysm (arrow) is treated by embolization.

To the Editor,

A 60-year-old male patient was admitted with abdominal pain, jaundice and nausea. His laboratory tests showed leukocytosis, anemia, prominent increase in liver function tests and hyperbilirubinemia. Alkaline phosphatase (709 U/l), lactate dehydrogenase (1141 U/l) and C-reactive protein (275 mg/L) values were very high. On ultrasonography (US) assessment, there was a heterogeneous lesion with hyper-hypoechoic internal structure including course calcification in liver left lobe. The gallbladder was not visualized in the normal anatomical localization. At this point, there was a well-defined, round cystic lesion including weak turbulent flow in B-mode US. Doppler US revealed no vascular coding in both cystic and heterogeneous lesions. MicroFlow imaging was applied to both lesions. In MicroFlow imaging, there was no vascularity in the heterogeneous lesion. However, the cystic lesion showed prominent vascular filling. The patient was diagnosed with gallbladder perforation, massive hematoma including pseudoaneurysm which is compatible with the cystic lesion. Computed tomography angiography (CTA) confirmed the diagnosis and cystic artery was realized as the source of the pseudoaneurysm. Embolization was applied as treatment (fig 1).

Simultaneous tissue movement and slow blood flow show an overlap in conventional Doppler. There is a one-dimensional wall filter in conventional Doppler to reduce the motion artifacts. As a result, slow flow signals are reduced. However, in MicroFlow imaging, there is an adaptive algorithm analyzing the tissue movements. The movement artifacts are removed with a multidimensional filter and the slow blood flow can be imagined [1].

Cystic artery pseudoaneurysm is a rare pathology causing bleeding, hematoma, and biliary obstruction. Commonly, it can occur secondary to acute cholecystitis or cholecystectomy. It is thought that there is weaken-

Received 27.06.2024 Accepted 21.07.2024
Med Ultrason
2024, Vol. 26, No 3, 316-317, DOI: 10.11152/mu-4420,
Corresponding author: Isil Basara Akin
Dokuz Eylul University
Faculty of Medicine,
35340 Izmir, Turkey
E-mail: isilbasara@gmail.com
Phone: +905066913699

ing in the adventitia of artery because of inflammatory damage. Clip application, vascular erosion, or thermal injury during cholecystectomy procedure may be other reasons of pseudoaneurysm. CTA is used to confirm the diagnosis. Doppler US and magnetic resonance imaging are other imaging tools. As treatment, endovascular embolization is the most common choice [2].

In our case, the patient had no surgical history. We believe that the reason for the pseudoaneurysm was the gallbladder perforation due to cholecystitis. Hematoma at the left lobe of the liver occurred because of vascular leak from the pseudoaneurysm of the cystic artery. Although there was no flow in Doppler US, MicroFlow imaging showed prominent vascular flow compatible with the pseudoaneurysm. MicroFlow imaging will make significant contributions to the diagnosis in detecting vascular pathologies, especially in the presence of weak vascularity.

References

1. Sawatzki M, Burkart T, Baumeler S, et al. Ultrasound Doppler technique for the diagnosis of focal nodular hyperplasia - case series and systematic review. Med Ultrason. 2024;26:72-82.
2. Taghavi SMJ, Jaya Kumar M, Damodaran Prabha R et al. Cystic Artery Pseudoaneurysm: Current Review of Aetiology, Presentation, and Management. Surg Res Pract 2021;2021:4492206.

Cubital tunnel syndrome and stroke coincide – adding insult to injury

Mustafa Güngör Albayrak[1], Ahmad J. Abdulsalam[1,2], Murat Kara[1]

[1]Department of Physical and Rehabilitation Medicine, Hacettepe University Medical School, Ankara, Turkey, [2] Department of Physical Medicine and Rehabilitation, Mubarak Alkabeer Hospital, Jabriya, Kuwait

To the editor,

A 41-year-old male presented with right hand weakness and numbness for around three months after his ischemic stroke. Despite multiple physician follow-ups, the patient's complaints were neglected and referred to physiotherapy, as they were attributed to be sequelae of the stroke. On gross inspection, claw hand deformity was observed along with hypothenar atrophy and distal weakness in his intrinsic hand muscles, specifically in the 4th and 5th digits. Ultrasound examination was performed revealing an enlarged/hypoechoic ulnar nerve on the right side compared to the left side (fig 1). An electrodiagnostic study was also conducted, revealing decreased ulnar sensory and motor amplitudes on the right side along with delay of the motor conduction velocity at the proximal elbow segment. The patient was diagnosed with cubital tunnel syndrome, and an elbow splint was provided.

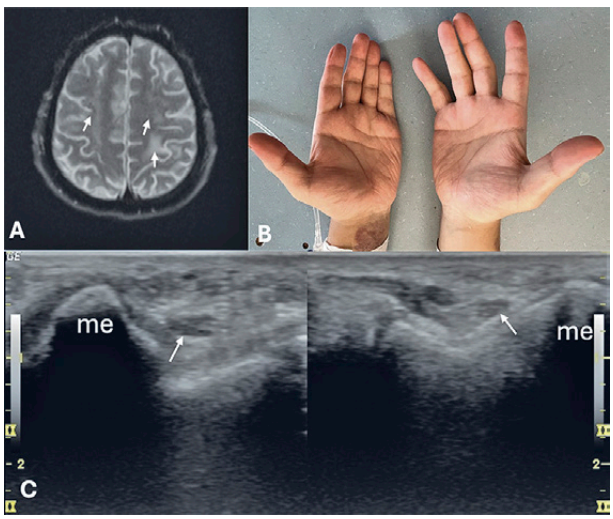

Fig 1. Axial magnetic resonance imaging of the brain showing diffusion restriction in both frontal lobes and left parietal lobe (A). Wartenberg's sign (abduction of the 5th digit) on the right hand (B). Comparative ultrasound examination of the elbow during semiflexion revealing a hypoechoic and enlarged ulnar nerve at the cubital tunnel (arrow) (C).

We present the case of entrapment neuropathy initially presumed to be secondary to stroke. While stroke can coincide with peripheral neuropathies, it is important to put in mind that stroke presentations can mimic peripher-

Received 05.06.2024 Accepted 21.07.2024
Med Ultrason
2024, Vol. 26, No 3, 317-318, DOI: 10.11152/mu-4421,
Corresponding author: Ahmad Jasem Abdulsalam
Department of Physical Medicine
and Rehabilitation
Mubarak Al-Kabeer Hospital, Kuwait
E-mail: dr.ahmad.j.abdulsalam@gmail.com

al neuropathies [1-3]. We also underscore the importance of the use of both electrodiagnostic and ultrasound examinations for the sake of reaching a prompt diagnosis, prognosis and treatment [4].

References

1. Lampl Y, Gilad R, Eshel Y, Sarova-Pinhas I. Strokes mimicking peripheral nerve lesions. Clin Neurol Neurosurg 1995;97:203-207.
2. Chapur J, Kojic K, Kula M, Flexman AM. Perioperative cortical hand stroke syndrome mimicking peripheral neuropathy: A case report. Can J Anaesth 2023;70:1839-1844.
3. Dozono K, Hachisuka A, Wada F, Hachisuka K. Peripheral neuropathies in nonparetic upper extremities of stroke patients induced by excessive use of a walking device. J Stroke Cerebrovasc Dis 2015;24:1841-1847.
4. Özçakar L, Kara M, Chang KV, et al. EURO-MUSCULUS/USPRM Basic scanning protocols for elbow. Eur J Phys Rehabil Med 2015;51:485-489.

The hidden menagerie of the posterolateral corner of the knee

Berkay Yalçınkaya[1], Ahmet Furkan Çolak[1], Ahmad Jasem Abdulsalam[1,2], Murat Kara[1]

[1]Hacettepe University Medical School, Department of Physical and Rehabilitation Medicine, Ankara, Turkey,
[2]Mubarak Alkabeer Hospital, Department of Physical and Rehabilitation Medicine, Jabriya, Kuwait

To the Editor,

We present two patients in their fifties who underwent ultrasound (US) examinations for their unilateral knee pain. The first patient also suffered from mild swelling and warmth in her left knee. The US examination demonstrated a hypoechoic, well-defined, septated cystic lesion in the posterolateral corner of her left knee (fig 1A). Magnetic resonance imaging (MRI) confirmed the same diagnosis of a paracapsular septated cyst, 2 cm in size, localized in the posterior vicinity of the popliteus tendon sheath (fig 1B). The cyst was drained and injected with corticosteroid under US guidance without complications.

The second patient presented with swelling and discomfort in his right knee. US examination revealed a few small loose bodies involving the popliteus tendon in the posterolateral corner of his right knee (fig 1C). MRI revealed several loose bodies within the popliteus tendon sheath and behind the posterior cruciate ligament (fig 1D). Since he did not describe knee pain, especially in the posterolateral aspect, he was treated conservatively with strengthening exercises.

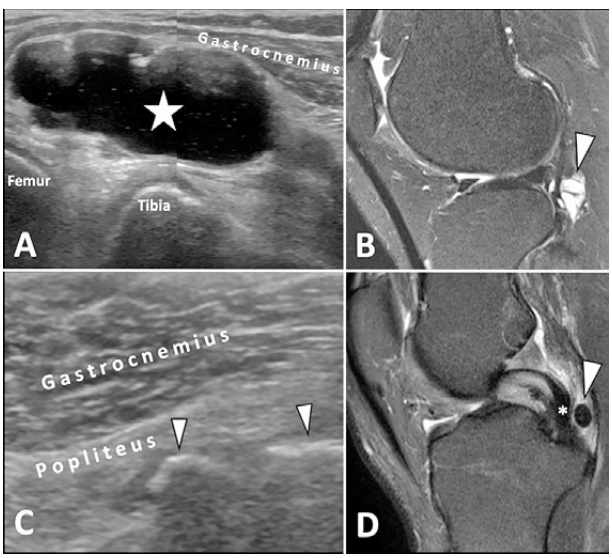

Fig 1. Ultrasound imaging demonstrates the hypoechoic, well-circumscribed cystic lesion (star) (A). Magnetic resonance imaging, proton density sagittal view, confirms the same cystic lesion as hyperintense (arrowhead) (B). Ultrasonographic imaging demonstrates the loose bodies (arrowheads) located within the popliteus tendon sheath (C). Magnetic resonance imaging, sagittal view, depicts another loose body (arrowhead) behind the posterior cruciate ligament (asterisk) (D).

Received 30.05.2024 Accepted 16.07.2024
Med Ultrason
2024, Vol. 26, No 3, 318-319, DOI: 10.11152/mu-4422,
Corresponding author: Berkay Yalçınkaya
Hacettepe Üniversitesi Tıp
Fakültesi Hastaneleri
Zemin Kat, FTR AD,
Sıhhıye Ankara,
Turkey, 06230
Phone/fax: +90 312 3094142
+90 312 3105769
E-mail: berkay0lka@gmail.com

Posterolateral corner (PLC) is a complex anatomical region of the knee and its pathologies are mostly associated with traumatic injuries, but biomechanical degenerative changes should not be overlooked such as loose bodies and cysts. One of the major static stabilizers of the PLC is the popliteus tendon, and loose bodies/calcifications, and cysts involving the popliteus tendon can rarely be seen, as in our two patients. Herein, we present two cases of knee pain with different pathologies in the posterolateral corner. Often termed the "dark side of the knee" due to the poor understanding of its structures, the posterolateral corner of the knee is not commonly scanned in every knee US protocol necessitating a high index of suspicion [1]. Although MRI can be used to diagnose relevant cases, US may be more convenient for use due to its multitudinous qualities, including handiness, low-cost, radiation-free, and dynamic assessment [2]. In addition, in terms of some pathologies such as cysts, it can be a convenient imaging tool to both help and treat the pertinent pathologies. To this end, especially in the case of the knee joint - which is quite common in the literature - this area should not be forgotten as part of the scanning protocol for US reassurance. Last but not least, we reiterate the point that the eventual medical decision of how to treat the patient should be based on symptomatology, as well as clinical and imaging findings.

References

1. Chahla J, Moatshe G, Dean CS, LaPrade RF. Posterolateral corner of the knee: Current concepts. Arch Bone Jt Surg 2016;4:97-103.
2. Özçakar L, Ricci V, Chang KV, et al. Musculoskeletal ultrasonography: ninety-nine reasons for physiatrists. Med Ultrason 2022;24:137-139.

A rare case of ovarian hypercalcemia type small cell carcinoma

Bin Hu[1,2], Yanan Li[2,3], Xin Li[2], Ming Zhang[2], Yi Jiang[2], Miao Shi[2]

[1]Shandong First Medical University and Shandong Academy of Medical Sciences, Jinan, [2]Department of Ultrasound, Liaocheng People's Hospital, Liaocheng, [3]School of Medical Imaging, Shandong Second Medical University, Weifang, Shandong, China

To the Editor,

A 42-year-old woman was admitted due to abdominal distension. She had a history of breast cancer and hysteromyoma. According to ultrasound assessment, there was a 15.0×14.7×9.8 cm cystic-solid mass in the pelvic cavity (fig 1a) with detectable arterial and venous blood flow signals within the mass. After surgical resection, the mass had a grayish-red nodular aspect (fig 1b). Pathological examination showed that the cells were arranged in a nest like, sheet-like, and follicular shape, with obvious atypia, consistent with (right adnexal region) malignant tumor. Immunohistochemical examination showed SMARCA4/Brg1 (-), suggesting ovarian hypercalcemia type small cell carcinoma (OSCCHT). Postoperatively, the patient received intravenous chemotherapy with cisplatin and etoposide.

OSCCHT is a rare ovarian malignancy, mainly occurring in women under the age of 40. The tumor was first described by Robert Scully in 1979 [1]. To date, fewer than 500 cases of OSCCHT have been reported globally [2]. Recent studies have revealed that changes of SMARCA4 gene are the main driving factor for the development of SCCOHT [3]. The gene is on chromosome 19. It encodes a protein, BRG1, which is immunohistochemically underexpressed. The SMARCA4 serves as a marker for the diagnosis of OSCCHT [4]. Due to paracrine effects of tumor cells, parathyroid hormone-related protein (PTH-rp) is produced to promote the release of bone calcium into the blood, resulting in elevated blood

Received 31.05.2024 Accepted 16.07.2024
Med Ultrason
2024, Vol. 26, No 3, 319-320, DOI: 10.11152/mu-4423,
Corresponding author: Miao Shi
Department of Ultrasound,
Liaocheng People's Hospital,
67 Dongchang West Road,
Dongchangfu District,
Liaocheng 252000,
Shandong,
China
Phone: 0635-8272300
E-mail: shimiaoemail@163.com

calcium. Patients often have symptoms associated with a pelvic mass, and only 1/3 of patients present with hypercalcemia [5]. SCCOHT progresses rapidly and is prone to recurrence; surgical treatment combined with adjuvant chemotherapy is the treatment of choice.

The ultrasound features of SCCOHT are unremarkable and easily confused with other gynecological tumors and gastrointestinal diseases. SMARCA4 gene expression deletion provides a great help in the diagnosis of SCCOHT, and the blood calcium level has reference value. How to quickly diagnose and treat the disease has become a constantly challenging hot topic for scholars at home and abroad.

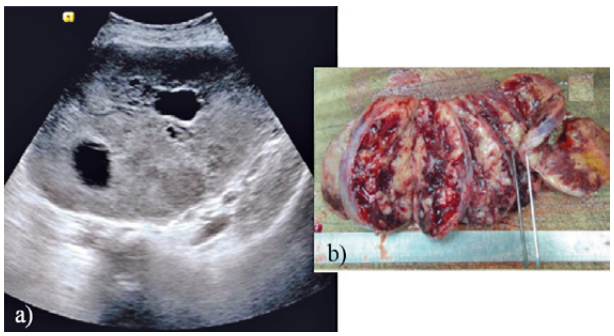

Fig 1. a) Ultrasound shows a cystic-solid mass in the pelvis with clear borders, predominantly solid, with the solid parts of the echoes being uneven in intensity and nodular in appearance; b) The right ovary is seen grossly as a greyish-red nodular pattern with a mostly intact peritoneum and local hemorrhage and edema.

References

1. Scully RE. Treatment of ovarian teratoma. Am J Obstet Gynecol 1979;135:161-162.
2. Tischkowitz M, Huang S, Banerjee S, etc. Small-Cell Carcinoma of the Ovary, Hypercalcemic Type-Genetics, New Treatment Targets, and Current Management Guidelines. Clin Cancer Res 2020;26:3908-3917.
3. Wens FSPL, Hulsker CCC, Fiocco M, et al. Small Cell Carcinoma of the Ovary, Hypercalcemic Type (SCCOHT): Patient Characteristics, Treatment, and Outcome-A Systematic Review. Cancers (Basel) 2023; 15:3794.
4. Yi G, Mingyi K, Hui W, et al Comprehensive treatment and genetic counseling for a SMARCA4 germline variant of ovarian hypercalcemia type small cell carcinoma. Chinese Journal of Cancer 2022;32:1115-1120.
5. Hongyu Z, Haoran L, Xi C, et al Clinical analysis and literature review of 11 cases of ovarian hypercalcemia type small cell carcinoma. Chinese Journal of Cancer 2021;31:136-142.

Ultrasonographic and pathological features of primary adrenal lymphoma

Qingkai Meng[1], Xiaoli Cao[2], Xintong Yu[3]

[1]Binzhou Medical University, Department of Ultrasound Medicine Binzhou, [2]Qingdao University Medical College Affiliated Yantai Yuhuangding Hospital, Department of Ultrasound, Yantai City, [3]Shandong Second Medical University, Department of Ultrasound Medicine, Weifang, Shandong, China

To the Editor,

A 59-year-old male presented with bilateral adrenal masses persisting for 24 days, accompanied by abdominal pain and low-grade fever, which worsened 3 hours prior to admission. On admission, the patient exhibited a low fever with a maximum temperature of 37.9°C. Ultrasonographic examination revealed hypoechoic masses in both adrenal regions (fig 1); the left mass measured approximately 9.4×3.9 cm and the right mass approximately 8.5×4.9 cm, both with clear boundaries, irregular shapes, and heterogeneous internal echoes. Color Doppler flow imaging (CDFI) did not detect any internal blood flow signals, and contrast-enhanced ultrasound (CEUS) showed rapid, uneven arterial phase enhancement of the adrenal masses with an enhancement intensity lower than that of the splenic parenchyma, followed by

Received 09.06.2024 Accepted 16.07.2024
Med Ultrason
2024, Vol. 26, No 3, 320-321, DOI: 10.11152/mu-4424,
Corresponding author: Xiaolo Cao
Qingdao University Medical College Affiliated Yantai Yuhuangding Hospital,
Department of Ultrasound
20 Yuhuangding East Road, Zhifu District,
Yantai City, Shandong Province, China
E-mail: xiaolic969@163.com

rapid washout in the venous phase. No enlarged lymph nodes were found in the cervical, axillary, or inguinal regions. A biopsy of the left adrenal mass was performed under ultrasound guidance using a 16G biopsy needle, obtaining three tissue samples for analysis. Immunohistochemistry revealed positive results for LCA, diffuse positive for CD20, sparse positive for CD3, positive for Pax-5, strong positive for P53 (80%), moderate positive for BCL-2 (80%), moderate positive for c-myc (60%), and approximately 80% positive for Ki-67. Considering the absence of extranodal lymphoma history and no involvement of other organs, the patient was ultimately diagnosed with primary adrenal lymphoma (PAL), specifically diffuse large B-cell lymphoma, not otherwise specified (NOS). Subsequently, the patient underwent treatment with the R-CHOP regimen.

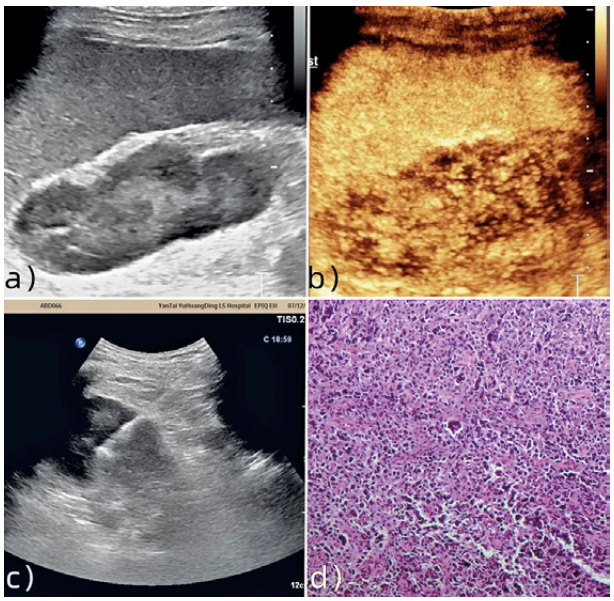

Fig 1. a) The lesion demonstrates clear boundaries with heterogeneous internal echogenicity and lacks significant blood flow signals; b) Contrast-enhanced ultrasound illustrates uneven enhancement within the lesion; c) Under ultrasound guidance, a 16G biopsy needle was used to perform a percutaneous biopsy on a left adrenal mass; d) Microscopic examination reveals a diffuse infiltration of medium-sized tumor cells, which are elliptical or round in shape, featuring vesicular nuclei with fine chromatin (HE×200).

The adrenal glands, located in the retroperitoneum, inherently lack lymphatic tissue; therefore, PAL is exceptionally rare, accounting for only 0.3% of all adrenal tumors [1]. Due to its retroperitoneal position, PAL often presents with nonspecific clinical symptoms, making it highly susceptible to misdiagnosis. Patients exhibiting unexplained fatigue, abdominal pain, and fever should undergo timely imaging examinations such as ultrasound to establish a definitive diagnosis [2].

The diagnosis of PAL necessitates a thorough exclusion of other adrenal-related conditions, and histopathological assessment is fundamental for confirmation. Given that PAL lacks characteristic radiological features, ultrasound-guided percutaneous biopsy plays a critical role in the definitive diagnosis of such cases [3].

References

1. Yu K, Xie W, Zhao L et al. sIL-2R: A Novel Diagnostic Biomarker for Primary Adrenal Lymphoma. J Clin Endocrinol Metab 2022;107:e2284-e2290.
2. Papageorgiou SG, Mavroeidi I, Kostakis M, et al. Primary Adrenal Lymphomas with Cushing's Syndrome: Two Cases with Evidence of Endogeneous Cortisol Production by the Neoplastic Lymphoid Cells. J Clin Med, 2023;12:5032.
3. Zeng J, Yan F, Chen Y, et al. Primary Adrenal Lymphoma: Two Case Series From China. Front Endocrinol (Lausanne) 2021;12:778984.

A case of scapular metastasis from hepatocellular carcinoma

Chengfang Yu*, Shuang Wang*, Na Shi, Li Li, Yilan Piao

**the authors share the first authorship*

Department of Medical Ultrasound, Yanbian University Hospital, Yanji 133000, Jilin, China

To the Editor,

A 59-year-old male patient was admitted with the chief complaint of "post-hepatocellular carcinoma (HCC) surgery for more than 4 years, and the discovery of a subcutaneous mass on the right shoulder for 4 months". Physical examination revealed a large mass of 20x20 cm on the right shoulder, with pain and tenderness upon palpation (fig 1a). The serum AFP level was 6,831 ng/ml. Ultrasound examination showed a huge mixed echo behind the right scapula. The size was 16.9x19.6x13.3cm, with unclear boundaries and no obvious capsule, the internal echo was uneven, and a disorderly distributed hyperechoic band could be seen within it (fig 1b). The scapula was disorganized, partially indistinct (fig 1c), mixed echo-probing and point-stripe blood flow signals (fig 1d). Ultrasound diagnosis: solid space-occupying lesion in the right shoulder, possible malignant bone tumor. Needle biopsy: metastatic cancer, consistent with the transfer of HCC according to immunohistochemistry and medical history.

HCC is the most common type of primary liver cancer, and the most common extrahepatic metastatic site is the lung, followed by lymph nodes and bone [1]. As the survival time of patients extends, the incidence of bone metastasis also increases, accounting for about 25% to 37% [2]. The most common site of bone metastasis is the axial skeleton (vertebrae, ribs, etc.) [3]. Metastases to the scapula are rarely reported. In this case, the sonographic appearance of bone metastatic cancer generally shows a heterogeneous echo soft tissue mass formed around the affected bone, with no obvious capsule, irregular bone destruction, and discontinuity of the bone cortex, with dot-like and strip-like blood flow signals that can be detected, which is consistent with the malignant manifestations described in previous literature [4]. When a patient has a soft tissue mass in the shoulder with osteolytic changes on ultrasound, in addition to malignant fibrous histiocytoma, synovial sarcoma, and clear cell sarcoma of soft tissue, the possibility of scapular metastasis of malignant tumors should be considered in combination with the patient's medical history.

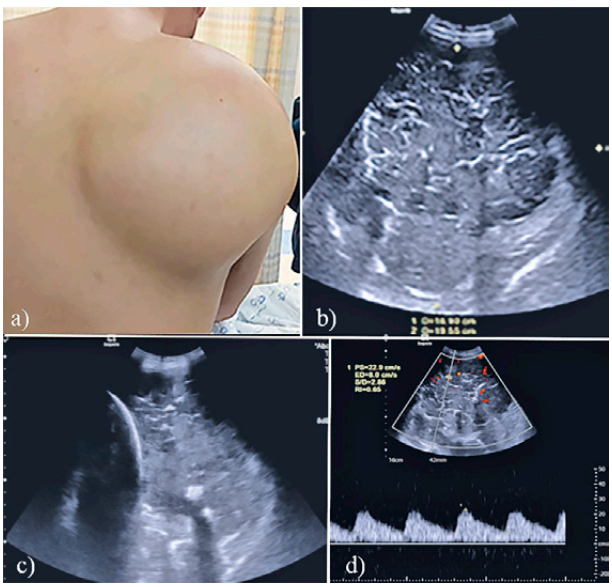

Fig 1. a) Physical examination revealed a large mass in the right shoulder; b) Ultrasound showed a huge mixed echo posterior to the scapula, and a hyperechoic band with disordered distribution was seen inside; c) Cortical interruption of scapula with unclear display; d) CDFI: Spot and stripe blood flow signal in soft tissue mass, RI:0.65.

Received 27.06.2024 Accepted 24.07.2024
Med Ultrason
2024, Vol. 26, No 3, 322-323, DOI: 10.11152/mu-4425,
Corresponding author: Yilan Piao
Department of Medical Ultrasound
Yanbian University Hospital
#1327 Juzi St. Yanji 133000, China
E-mail: 1419299989@qq.com

References

1. Katyal S, Oliver J H, 3rd, Peterson MS, et al. Extrahepatic metastases of hepatocellular carcinoma. Radiology 2000;216:698-703.
2. Uchino K, Tateishi R, Shiina S, et al. Hepatocellular carcinoma with extrahepatic metastasis: clinical features and prognostic factors. Cancer 2011;117:4475-4483.

3. Kim KH, Oh HH, Son DJ, et al. Scapular metastasis of hepatocellular carcinoma presenting as acute bleeding and hematoma: A case report of safe and effective treatment. Medicine (Baltimore) 2017;96:e8736.

4. Madej T, Flak-Nurzyńska J, Dutkiewicz E, et al. Ultrasound image of malignant bone tumors in children. An analysis of nine patients diagnosed in 2011-2016. J Ultrason 2018;18:103-111

Ultrasound-guided proximal-anterior axillary nerve block: a novel technique

Akiko Hata[1], Makoto Sato[2], Takayuki Kunisawa[1]

[1]Department of Anesthesiology, Tokyo Nishi Tokushukai Hospital, [2]Department of Anesthesiology, Tokyo Metropolitan Children's Medical Center, Tokyo, Japan

To the Editor,

The axillary nerve block provides shoulder pain relief and can be used in the diagnosis and treatment of quadrilateral space syndrome [1]. The axillary nerve originates in the posterior cord of the brachial plexus, and ultrasound-guided injection through the posterior shoulder is commonly performed [2]. However, this approach does not ensure that the solution spreads proximally along the axillary nerve without becoming entrapped before entering the quadrilateral space. The present report describes a novel, proximal-anterior approach for ultrasound-guided, axillary nerve block.

The technique

The subject is placed in a comfortable, supine position with the upper extremities turned to the side so as not to extend the nerves of the brachial plexus and isolate them. A transducer is then superimposed from the head of the humerus toward the ipsilateral nipple (fig 1A). The ultrasound image shows the pectoralis major muscle at the top, the musculocutaneous nerve between the short head of the biceps brachialis muscle and coracobrachialis muscle, and the subscapularis muscle positioned obliquely (fig 1B). The axillary nerve runs away from the axillary artery and the nerve cords surrounding the coracoid process and passes through the quadrilateral space with the posterior brachial circumflex artery. Before entering the quadrilateral space, the axillary nerve can be visualized as a hyperechoic image behind and cephalad to the axillary artery above the subscapularis muscle (Fig 1B). The needle is inserted into the plane laterally to medially on the surface of subscapularis muscle using a peripheral nerve stimulator (1 mA, 0.1 ms, and 2 Hz) to exclude the radial nerve originating in the posterior cord of the brachial plexus. Needle insertion is guided by ultrasound until either contact of the needle with the axillary nerve or contraction of the deltoid muscle is elicited while titrating with the current at 0.5 and 0.8 mA. The injected solution allows the axillary nerve to be hydro-

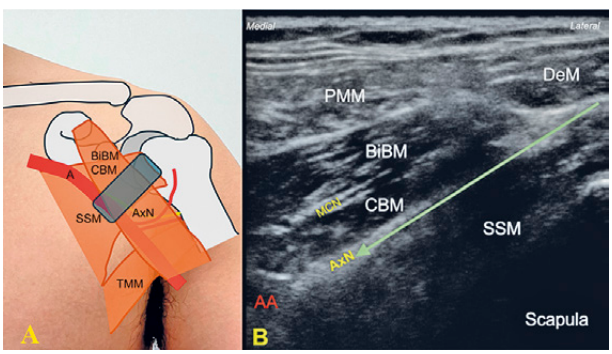

Fig 1. Illustration of the neuromuscular anatomy removing the pectoralis major and deltoid muscles (A) and sonoanatomy of the anterior proximal axilla (B). BiBM, biceps brachialis muscle; CBM, coracobrachialis muscle; SSM, subscapularis muscle; TMM, teres major muscle; AA, axillary artery; AxN, axillary nerve; PMM, pectoralis major muscle; DeM, deltoid muscle; MCN, musculocutaneous muscle. The gray rectangle indicates the transducer's position. The green arrow shows the path of the inserted needle.

Received 04.06.2024 Accepted 17.07.2024
Med Ultrason
2024, Vol. 26, No 3, 323-324, DOI: 10.11152/mu-4426,
Corresponding author: Akiko Hata
Department of Anesthesiology,
Tokyo Nishi Tokushukai Hospital,
3-1-1 Matsubaracho,
Akishima, Tokyo 196-0003, Japan
E-mail: aqua42232@gmail.com

dissected along its short axis above the subscapularis muscle.

Selective axillary nerve block can be achieved with around 5cc of the drug solution using this approach because the other terminal nerves and cords move away from each other laterally toward the coracoid process; even single-injection infraclavicular brachial plexus block has a relatively high incidence of incomplete posterior cord block [3]. Since this is a relatively deep procedure, a low-frequency ultrasound probe (convex type) should be used depending on the patient's physique. This technique is useful for ambulatory treatment; it causes little discomfort to the patient because the affected upper limb does not need to be abducted, no muscles need to be penetrated, and the procedure can be easily used in combination with subacromial bursal injections.

References

1. Chen H, Narvaez VR. Ultrasound-Guided Quadrilateral Space Block for the Diagnosis of Quadrilateral Syndrome. Case Rep Orthop 2015:2015:378627.
2. Rothe C, Asahara S, Andersen HL, et al. Ultrasound-guided block of the Axillary nerve: A volunteer study of a new method. Acta Anaesthesiol 2011;55:565-70.
3. Sun-Kyung P, Su-Young L, Won Ho K, et al. Comparison of Supraclavicular and Infraclavicular Brachial Plexus Block: A Systemic Review of Randomized Control Trials. Anesth Analg 2017;124:636-44.

Ultrasound findings of non-Hodgkin's mantle cell lymphoma in the right inguinal region

Haotian Zhao[1,2], Xiaona Wang[1], Yaru Yan[2,3], Li Li[1]

[1]Department of Ultrasound, Hebei General Hospital, [2]Hebei Medical University, [3]Department of Ultrasound, Shijiazhuang People' Hospital, Shijiazhuang, Hebei, China

To the Editor,

A 56-year-old male came to the ultrasound department for an ultrasound (US) examination. We found a raised mass in his right inguinal region. This mass did not disappear with changes in position and palpation. The patient reported that the mass has been around for over 4 years and now feels larger than before.

The US examination showed multiple abnormal lymph nodes in the subcutaneous soft tissue of the right inguinal region, among which the larger hypoechoic mass was of the size 59.9×78.2×44.7mm, with uneven internal echo **(**fig 1a**)**. The color Doppler mode displays approximately circular and bar shaped blood flow signals (fig 1b). The use of two-dimensional shear wave elastography (SWE) to examine the package showed an average Young's modulus value of 6.64 kPa (fig 1c). We reviewed the patient's medical records system after examination. The immunohistochemical staining: CD3(-), CD43(-), CD20(+), CD79α(+), CD21(FDCnetwork+), Ki-67(approximately 30%+), BcL-2(+), Bcl-6(-), CD10(-), Cyclin D1(+), CD23(FDCnetwork+), SOX-11(+), CD30(+) (fig 1d). The result was consistent with the histopathological diagnosis of non-Hodgkin's mantle cell lymphoma (MCL). Computed tomography (CT) also showed a mass in the right inguinal region (fig 1e).

MCL is an aggressive subtype of non-Hodgkin lymphoma characterized by the t(11;14) chromosomal translocation and overexpression of cyclin D1 [1]. There are significant differences in clinical manifestations, pathological features, treatment, and prognosis between mantle cell lymphoma and other types of B-cell lymphoma. NCL accounts for approximately 6%~8% of non-Hodgkin's lymphoma and is more common in the elderly, with more male patients than females [2]. The preferred examina-

Received 02.07.2024 Accepted 24.07.2024
Med Ultrason
2024, Vol. 26, No 3, 324-325, DOI: 10.11152/mu-4427,
Corresponding author: Li Li
Department of Ultrasound,
Hebei General Hospital
348 Heping West Road,
Shijiazhuang, 050051 Hebei,
China
E-mail: shrmgnk@126.com

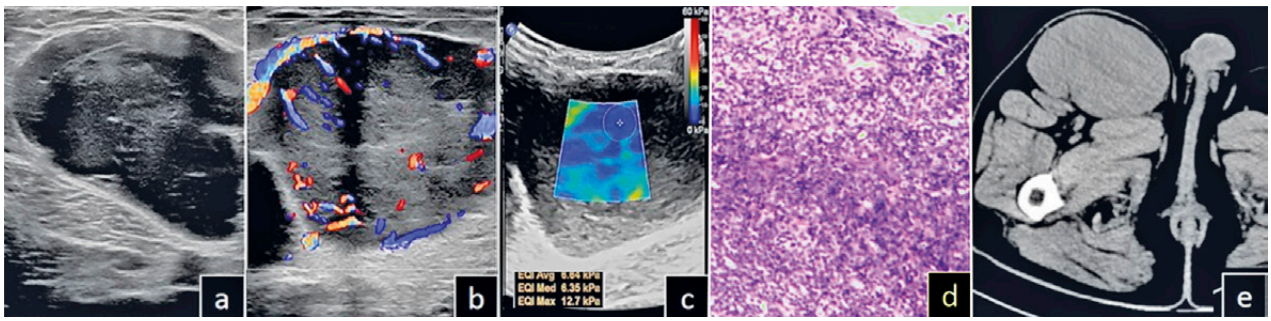

Fig 1. a) Ultrasound aspect of a hypoechoic mass in the right inguinal region; b) Color Doppler showed approximately circular and bar shaped blood flow signals; c) two-dimensional shear wave elastography showed an average Young's modulus value of 6.64 kPa; d) the histopathological images showed proliferative lesions in lymphoid tissue (HE×200); e) Computed tomography (CT) showed a mass in the right inguinal region.

tion method for detecting MCL in the inguinal region is US. The mass usually appears elliptical and exhibits non-homogeneous echostructure, with color Doppler showed substantial blood flow signals [3]. Malignant nodes often tend to be round, while benign lymph nodes are characterized by an oval shape [3]. The two-dimensional SWE imaging can measure the stiffness and uniformity of the mass. Additionally, US-guided puncture biopsy is helpful for diagnosing MCL.

References

1. Lymphoma Research Foundation LRF. Twenty years of advancing discoveries and treatment of mantle cell lymphoma. Oncology 2024;38:51-67.
2. Cheah CY, Seymour JF, Wang ML. Mantle Cell Lymphoma. J Clin Oncol 2016;34:1256-1269.
3. Cocco G, Boccatonda A, D'Ardes D, et al. Mantle cell lymphoma: from ultrasound examination to histological diagnosis. J Ultrasound 2018;21:339-342.

An interesting mass: a case of abdominal teratoma from ovary complicated with torsion

Shuang Zheng[1*], Fang Peng[1*], Chengwen Tong[2], Dawei Wang[3], Lian-di Liu[1], Bin Xiao[1]

[*]the authors share the first authorship

[1]Department of Ultrasound, [2]Department of Radiology, [3]Department of Ultrasound, Taihe Hospital, Hubei University of Medicine, Shiyan, China

To the Editor,

A 58-year-old female was admitted with intermittent pain in the right upper abdomen for 3 months. The tenderness of the right upper abdomen was obvious, and a mass could be palpated. Blood routine, tumor markers (such as CA-125), and stool routine were normal.

Abdominal ultrasound detected a mixed echo mass (11.2×8.5 cm) in the right upper abdomen, with clear boundary, regular shape, uneven internal echo, and with no blood flow signal (fig 1A,B). The cystic mass in the right upper abdomen was suggested to be a teratoma. Contrast-enhanced CT showed a mixed lipoid density tumor (99×79 mm) in the right upper abdomen with soft tissue nodules and calcifications. A banded soft tissue was connected with the right appendix. The mass was not obviously reinforced (fig 1C, D).

Received 23.06.2024 Accepted 21.07.2024
Med Ultrason
2024, Vol. 26, No 3, 325-326, DOI: 10.11152/mu-4428,
Corresponding author: Bin Xiao MD
Department of Ultrasound,
Renmin Hospital,
Hubei University of Medicine,
Shiyan 442000, Hubei, China
E-mail: 7771563@qq.com

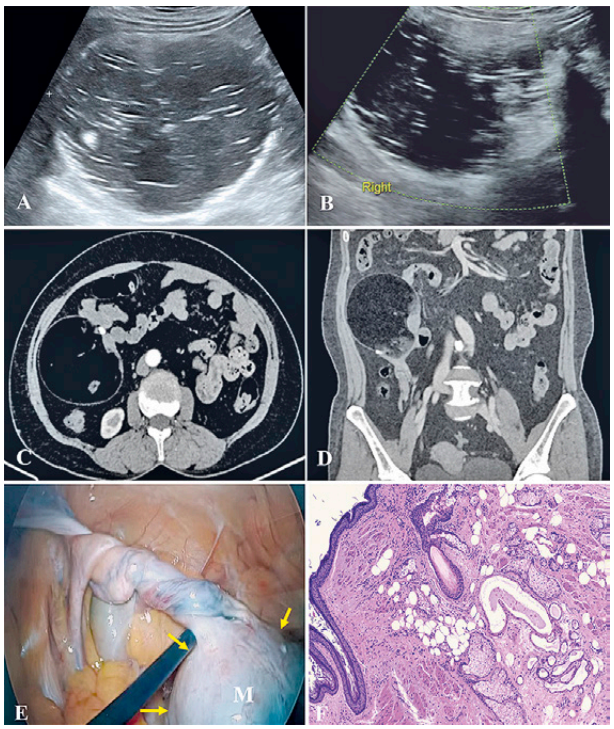

Fig 1. A) Ultrasound detected a mixed echo mass in the right upper abdomen, with clear boundary, regular shape, and uneven internal echo. The cystic part of the mass was unclear with multiple short-line hyperechoes and patchy hyperechoes in the cyst wall; B) There was no blood flow signal detected in the mass; C) Contrast-enhanced CT showed a mixed lipoid density tumor in the right upper abdomen with soft tissue nodules and calcifications; D) A banded soft tissue was connected with the right appendix; E) A huge mass was seen in the right upper abdomen and a pedicle connected it to the right ovary with three times twisted during the surgery; F) Pathology confirmed the diagnosis of a mature cystic teratoma of the right ovary. M: Mass.

During surgery, a huge mass was seen in the right upper abdomen and a pedicle connected it to the right ovary which was twisted three times (fig 1E). Pathology confirmed the diagnosis of a mature cystic teratoma of the right ovary (fig 1F).

Ovarian teratoma is a common germ cell tumor which has no obvious symptoms in the early stage [1]. A few patients may have symptoms such as abdominal distension, abdominal pain, and abdominal mass [2]. Ovarian teratomas are mostly located in the pelvic adnexal area. In this case, it is rare that the mass was located in the upper abdomen. Because of the long pedicle of the mass, it has great mobility and twists with the change of body position which makes the patient have symptoms such as abdominal pain and bloating. Huge mature cystic teratoma in the abdominal cavity is rare. Because the patient was obese, the display of twisted pedicle was not clear which led to the missed diagnosis of torsion. Fortunately, the patient in this case received timely surgical treatment and the prognosis was good.

Acknowledgments: The work was supported by Shiyan Science and Technology Bureau of Hubei Province (No. 22Y60)

References

1. Opalinska M, Sowa-Staszczak A, Olearska H, et al. Clinical Approach to Neuroendocrine Neoplasm Associated With Ovarian Teratoma. Front Endocrinol (Lausanne), 2021;12:770266.
2. Lee Y L, Lai C R, Yen M S. Recurrent ovarian mixed germ cell tumor with unusual malignant transformation: a case report. J Ovarian Res, 2019;12:2.

Comment to: Perfluorobutane (Sonazoid) Contrast-enhanced ultrasound to diagnose hepatocellular carcinoma: A systematic review and meta-analysis

Ke Xu

Ultrasound Department, The Second Affiliated Hospital of Chengdu Medical College, Chengdu, China

To the Editor,

I read with interest the study of Chen et al [1] published in Med Ultrason. After a thorough review of the manuscript, several discrepancies and methodological issues have been identified that I believe warrant attention and further discussion.

Firstly, there is a misalignment between the stated research objectives and the actual contents of the study. The title and introduction of the article focus on evaluating Sonazoid CEUS diagnostic efficacy for hepatocellular carcinoma (HCC). However, the keywords used in the search strategies included terms such as "cholangiocarcinoma," "liver adenoma," and even "liver abscess," indicating a broader scope of research but only 14 studies were involved and included some studies with quite a small sample size. Nevertheless, there's another meta-analysis by Ren et al yielded 30 studies with similar objectives [2], which raises concerns about the selection criteria and reasons for excluding certain studies. Besides, some studies enrolled in the article had different objectives, like "for diagnosis of recurrent HCC" [3]. Furthermore, the discussion within the manuscript which delved into assessing liver metastases, also deviated from the study's defined objectives.

Secondly, there are several methodological issues that need to be addressed. The criteria for diagnosing Sonazoid are different across different studies referenced in the manuscript, including the ACR LI-RADS 5 criteria, arterial phase hyperenhancement (APHE) and the wash out of Kupffer phase standards, modified LI-RADS 5 criteria and even with two of them [4] (then which result of the two standards should be applied?). How were biases resulting from these differences controlled? In addition, several studies were based on quite small numbers of sample size. Also, it's not appropriate to administer multiple contrast injections in one examination as it's not recommended within the Sonazoid's product manual.

Lastly, the inclusion of a comparison between Sonazoid and another ultrasound contrast agent, SonoVue, is outside the scope of the study's objectives too. Besides, the meta-analysis only included 4 studies involving SonoVue, making it inappropriate to conclude that Sonazoid is comparable to SonoVue. Moreover, there are published comprehensive meta-analyses [2] and reviews [5] which have indicated that APHE and late washout are more frequently observed with SonoVue than with Sonazoid, highlighting a significant discrepancy with the conclusions drawn in this article.

Therefore, we suggest further illustration of these issues to avoid subjective bias of the evaluation of Sonazoid CEUS to diagnose HCC.

Received 16.06.2024 Accepted 15.07.2024
Med Ultrason
2024, Vol. 26, No 3, 327, DOI: 10.11152/mu-4429,
Corresponding author: Ke Xu
Ultrasound Department, The Second Affiliated Hospital of Chengdu Medical College, Chengdu, China
E-mail: xuke808080@163.com

References

1. Chen Y, Zhu W, Yi Y, et al. Perfluorobutane (Sonazoid) Contrast-enhanced ultrasound to diagnose hepatocellular carcinoma: A systematic review and meta-analysis. Med Ultrason 2024;26:187-196.
2. Ren J, Lu Q, Fei X, et al. Assessment of arterial-phase hyperenhancement and late-phase washout of hepatocellular carcinoma-a meta-analysis of contrast-enhanced ultrasound (CEUS) with SonoVue® and Sonazoid®. Eur Radiol. 2023;34:3795-3812.
3. Shagdarsuren B, Tamai H, Shingaki N, et al. Contribution of Contrast-Enhanced Sonography With Perfluorobutane Microbubbles for Diagnosis of Recurrent Hepatocellular Carcinoma. J Ultrasound Med 2016;35:1383-1391.
4. Hwang JA, Jeong WK, Kang HJ, et al. Perfluorobutane-enhanced ultrasonography with a Kupffer phase: improved diagnostic sensitivity for hepatocellular carcinoma. Eur Radiol 2022;32:8507-8517.
5. Barr RG, Huang P, Luo Y, et al. Contrast-enhanced ultrasound imaging of the liver: a review of the clinical evidence for SonoVue and Sonazoid. Abdom Radiol (NY). 2020;45:3779-3788.

Author's response

Yujia Chen, Wenjun Zhu, Yunyun Yi, Huali Cao, Fan Chen, Qinling Zhu

Department of Ultrasound, Affiliated Hospital of Jiaxing University, First Hospital of Jiaxing, Jiaxing, China

Dear Editor,

We appreciate the thoughtful review and constructive feedback provided by Dr Ku in evaluating our manuscript.

Our goal was to obtain the pool sensitivity and specificity so that we could clearly demonstrate the diagnostic efficacy of Sonazoid CEUS to diagnose HCC, so we needed to extract 2×2 contingency tables (true-positive (TP), false-positive (FP), true-negative (TN), and false negative (FN) from original articles. We included in our meta-analysis studies from which TP/FP/TN/FN could be extracted from original articles and meets other included criteria (details can be seen in the manuscript). Also, we tried to extract HCC data (TP/FP/TN/FN) from a study that covered all types of focal liver lesions. For example, the article by Luo (2010) [1] contains a variety of focal liver lesions (HCC, metastases, hemangiomas and FNHs); however, we could extract the TP/FP/TN/FN related to HCC. Another reason is that Sonazoid is only available in a few countries. Therefore, the data is not as comprehensive as SonoVue. We wanted to obtain all the relevant data about Sonazoid CEUS for diagnosing HCC, thus improving the credibility of our meta-analysis. Therefore, the search terms are both extensive and specific.

We have read the review of SonoVue and Sonazoid mentioned by the reviewer [2], but the objective of this article is different from ours. The main focus of this review is on the CEUS features of SonoVue and Sonazoid, not on their ability to diagnose HCC. The results are the proportion of APHE and washout at late phase/KP with SonoVue was different with Sonazoid in this article. The conclusion mentions that APHE and late washout in HCC are more frequently observed with SonoVue than with Sonazoid. We believe that this conclusion has less relevance compared to ours. In other words, the two meta-analyses analyzed Sonazoid CEUS from different aspects.

Many of the articles included in Ren et al. study [2] were not available for us to extract data (TP/FP/TN/FN), so they were excluded. The details about regarding the reasons of exclusion are summarized in the supplementary Table I. In addition, the population in our study did not exclude patients with a history of liver cancer because we considered that the history of liver cancer was only a high-risk factor for the diagnosis of HCC, rather than an exclusion criterion. In our study, the population included in 8 articles was at high risk of HCC (supplementary Table II) due to HBV/HCV infection, liver cirrhosis, history of liver cancer, and other factors. The analysis was performed using a meta-regression analysis in the Table III. In conclusion, we believe that this article can be included in our study.

Although liver metastases are mentioned to enhance the content, they may deviate from the objective. However, it occupies only a small amount of space in the article.

The CEUS diagnostic criteria for Sonazoid in diagnosing HCC are still being updated, so when extracting the data, we selected the results considered best by the authors. From a methodological point of view, diagnostic criteria may be one of the causes of heterogeneity, but unfortunately, two articles did not mention diagnostic criteria which made it impossible to analyze them in the regression analysis. We used sensitivity analysis, subgroup analysis, and meta-regression to ensure our study was as credible as possible in terms of methodological aspects. Moreover, the use of LI-RADS was examined in meta-regression analysis (Table III). Comparing the revised LI-RADS and ACR versions in the supplementary material is due to this reason. The details of diagnostic criteria for HCC are summarized in Table II.

The included articles involved 4 studies that directly compared SonoVue and Sonazoid for the diagnosis of HCC, with the same nodules being examined using both SonoVue and Sonazoid contrast agents. We are of the opinion that these data can be summarized as well. For example, an article published in Radiology [3], the authors conducted a subgroup analysis of articles that directly compared the diagnostic accuracy of cardiac MRI versus FDG PET for Cardiac Sarcoidosis (only six studies that evaluated both modalities in the same patients), which is similar to ours. Furthermore, we conducted a comparative analysis with other meta-analyses that included all types of contrast agents, including SonoVue. We believe that our conclusions are appropriate and meaningful, Sonazoid being comparable to Sonovue in HCC diagnosis. We would like to emphasize that our

analysis does not involve specific contrast features like the performance in different vascular phases of CEUS, but pooled sensitivity and specificity.

We sincerely appreciate the time and effort invested by Dr Ku in evaluating our manuscript. We look forward to any additional feedback or suggestions.

References

1. Luo W, Numata K, Morimoto M, et al. Differentiation of focal liver lesions using three-dimensional ultrasonography: retrospective and prospective studies. World J Gastroenterol 2010;16:2109-19.
2. Ren J, Lu Q, Fei X, Dong Y, et al. Assessment of arterial-phase hyperenhancement and late-phase washout of hepatocellular carcinoma-a meta-analysis of contrast-enhanced ultrasound (CEUS) with SonoVue® and Sonazoid®. Eur Radiol 2024;34:3795-3812.
3. Aitken M, Chan MV, Urzua Fresno C, et al. Diagnostic Accuracy of Cardiac MRI versus FDG PET for Cardiac Sarcoidosis: A Systematic Review and Meta-Analysis. Radiology 2022;304:566-579.